

Article

Design of Magnesia–Spinel Bricks for Improved Coating Adherence in Cement Rotary Kilns

Graziella Rajão Cota Pacheco ^{1,*}, Geraldo Eduardo Gonçalves ¹ and Vanessa de Freitas Cunha Lins ² 

¹ RHI Magnesita Research and Development Center, Contagem 32210-190, Brazil; geraldo.eduardogoncalves@contractor.rhimagnesita.com

² Chemical Engineering Department, Universidade Federal de Minas Gerais, Belo Horizonte 31270-901, Brazil; vlins@deq.ufmg.br

* Correspondence: graziella.pacheco@rhimagnesita.com

Abstract: It is well known that doloma bricks present better coating adherence than magnesia–spinel bricks when applied in cement rotary kilns, which is related to the different coating formation mechanism. The coating has an essential role in prolonged operation by protecting the refractory lining; thus, it is important to improve its adherence on magnesia–spinel refractories. The objective of this investigation is to study different compositions of magnesia–spinel bricks, achieved by varying additives used (calcined alumina, limestone, hematite and zirconia) and firing temperature (1500 °C and 1700 °C), to enhance the coating adherence measured by the sandwich test. The results have pointed out that the use of higher firing temperature contributes positively to physical adherence due to well-sintered refractory structure and elevated permeability, attaining coating strength superior to 2 MPa. For the chemical adherence, the addition of 2 wt.% of limestone increased the coating strength to 3 MPa, but resulted in a drop in hot properties. In this context, the most suitable approach to improve adherence of clinker coating and maintain hot properties in suitable levels is to increase the firing temperature.

Keywords: magnesia–spinel refractory brick; coating; improvement



Citation: Pacheco, G.R.C.; Gonçalves, G.E.; Lins, V.d.F.C. Design of Magnesia–Spinel Bricks for Improved Coating Adherence in Cement Rotary Kilns. *Ceramics* **2021**, *4*, 652–666. <https://doi.org/10.3390/ceramics4040046>

Academic Editors: Narottam P. Bansal and Gilbert Fantozzi

Received: 1 April 2021
Accepted: 19 November 2021
Published: 29 November 2021

Publisher's Note: MDPI stays neutral with regard to jurisdictional claims in published maps and institutional affiliations.



Copyright: © 2021 by the authors. Licensee MDPI, Basel, Switzerland. This article is an open access article distributed under the terms and conditions of the Creative Commons Attribution (CC BY) license (<https://creativecommons.org/licenses/by/4.0/>).

1. Introduction

Doloma and magnesia–spinel refractory bricks have increased their importance in cement rotary kilns since the hexavalent chrome issues associated with magnesia–chromite bricks became a major concern in the early 1980's [1–3]. Both refractories present high refractoriness and chemical compatibility to basic environments, what qualifies them for use in cement kilns. Despite the disadvantage of hydration presented by doloma bricks, the formation of a strongly adhered clinker coating onto these bricks is an important advantage when applied in the burning zone of cement rotary kilns [4]. The coating, which is a clinker layer adhered to the brick surface, has an important role in prolonged operation by protecting the refractory lining from chemical, thermal and abrasive wear, and reduced energy consumption in cement production [1,4,5].

The better coating adherence presented by doloma bricks compared to magnesia–spinel bricks is related to the different coating formation mechanism. Doloma refractory provide a large amount of CaO, which reacts with dicalcium silicate (C₂S) from clinker, leading to the formation of a tricalcium silicate (C₃S) rich zone at the clinker–brick interface, with a strong bonding between the clinker and the brick [1,2,5]. Therefore, the coating formation on doloma bricks does not require any excessive liquid phase formation [6]. On the other hand, the liquid phase formation is inherent to the mechanism of coating adherence on magnesia–spinel bricks, since spinel reacts with lime phases from clinker to form low refractoriness phases, such as mayenite (C₁₂A₇) and Q phase (Ca₂₀Al₂₆Mg₃Si₃O₆₈). The resulting liquid phase intensifies the clinker–brick interaction, but only a thin layer of dicalcium silicate is formed, as tricalcium silicate cannot coexist with spinel [3,5,6].

Many authors have studied the coating adherence on basic bricks [7–12]. Recently, the sandwich coating test has been applied in some studies [2,3,6,11,12]. Guo et al. [3] showed that the most significant effects on adherence strength of magnesia–spinel bricks are silica ratio ($SR = SiO_2 / Al_2O_3 + Fe_2O_3$) of the cement raw meal, heating rate of the sandwich test and particle size of the meal. Meng et al. [11] investigated the effect of zircon ($ZrO_2 \cdot SiO_2$) addition on coatability of $MgO-C_2S-C_3S$ refractory materials. According to the study, the highest adherence strength was obtained for 0.5 wt.% ZrO_2 addition because the dissolution of $CaZrO_3$ into the cement clinker increased the viscosity of the clinker and the bonding with the refractory. The sandwich test used by Lin et al. [12] supported their work about adherence properties of cement clinker on porous periclase–spinel refractory aggregates. It was observed that when the spinel content was 15–40 wt.%, the refractory aggregate had not only a high clinker corrosion resistance but also a high coating adherence.

In practice, a coating will form if the conditions in the kiln are appropriate. However, the composition and the microstructure of the refractory used are also important to determine the quality of the coating. Thus, the objective of this investigation is to study different compositions of magnesia–spinel refractory bricks to improve coating adherence: additives (calcined alumina, limestone, hematite and zirconia) and firing temperature (1500 °C and 1700 °C). It is expected that the addition of calcined alumina will influence the coating adherence due to the formation of fine spinel which easily reacts with clinker. Limestone and hematite were selected to ease the formation of liquid phase in the brick. The role of ZrO_2 is to react with CaO from the clinker, generating calcium zirconate ($CaZrO_3$), which is reported to promote the formation of a protective coating.

2. Materials and Methods

Five different magnesia–spinel brick compositions fired at two temperatures, as shown in Table 1, were prepared in the laboratory. The main raw materials used were high purity dead burned magnesia (DBM), with bulk density of 3.3 g/cm³ and MgO content of 98 wt.%, and fused spinel (MA), with bulk density of 3.4 g/cm³ and Al_2O_3 and MgO contents of 67 wt.% and 32 wt.%, respectively. Two percent of the four selected additives were added: calcined alumina (average particle size of 5 µm and purity of 99.6 wt.%), limestone <75 µm (average particle size of 23 µm and purity of 98.7 wt.%), CaO-partially stabilized zirconia <75 µm (average particle size of 12 µm and purity of 95.5 wt.%), and hematite <75 µm (average particle of size 41 µm and purity of 99.3 wt.%).

Table 1. Compositions of magnesia–spinel bricks produced at the laboratory.

Composition	DBM (wt.%)	MA (wt.%)	Additive	Firing Temperature (°C)
A-1	80	20	no	1500
A-2	78	20	calc. alumina	1500
A-3	78	20	limestone	1500
A-4	78	20	hematite	1500
A-5	78	20	zirconia	1500
A-6	80	20	no	1700
A-7	78	20	calc. alumina	1700
A-8	78	20	limestone	1700
A-8	78	20	hematite	1700
A-10	78	20	zirconia	1700

The compositions were prepared by mixing the raw materials with 3 wt.% of an organic binder solution for 15 min, in a roller mixer. Subsequently, 160 × 85 × 64 mm³ bricks were pressed using a laboratory hydraulic press at pressure of 210 MPa, and then dried at 120 °C for 12 h. The bricks were heat-treated under oxidizing conditions at 1500 °C for 5 h or 1700 °C for 5 h, in an electric muffle furnace.

After the heat treatment, the compositions were characterized in terms of bulk density (BD) and apparent porosity (AP) according to ISO 5017: 2015 standard; modulus of elasticity at room temperature (ME) according to ASTM C885 standard; cold crushing strength (CCS)

according to ISO 10059–Part 2: 2014 standard; hot modulus of rupture (HMOR) at 1200 °C and at 1485 °C for 3 h according to ISO 5013: 2012 standard; gas permeability according to ASTM C577 standard; chemical composition by X-ray fluorescence using the PW2540 Philips spectrometer; study of mineralogical composition by X-ray diffraction (XRD) using PANalytical equipment, X'Pert PRO model where the analysis was performed in the X'Pert HighScore Plus program using the JCPDS–International Centre for Diffraction Data as database; and microstructural observations by means of reflected light optical microscope of Zeiss, AXIO Imager.A1m model.

The evaluation of the coating adherence on the refractory bricks was based on the sandwich method described in the previous work [13]. For the coating agent, a cement raw meal was collected from a Brazilian cement producer and ground to achieve <75 µm. The typical properties of this meal are presented in Table 2. To prevent the transformation of $\beta\text{C}_2\text{S}$ into $\gamma\text{C}_2\text{S}$, which is accompanied by 10 to 12% volume expansion [14], thus prejudicial to the coating adherence upon cooling down the samples, 1 wt.% of boric acid was added to the cement meal. According to Zhao [14], chemical impurities, such as Na_2O , P_2O_5 , B_2O_3 , Cr_2O_3 and K_2O , are stabilizers of $\beta\text{C}_2\text{S}$, which justifies the use of boric acid.

Table 2. Properties of the cement raw meal used in the sandwich coating test.

Cement Raw Meal after Grinding		
Particle Size Distribution (µm)		
d ₉₈		124.0
d ₉₀		78.2
d ₇₅		44.7
d ₅₀		17.5
d ₂₅		5.6
d ₁₀		1.9
Chemical composition (wt.%)		
CaO		66.7
SiO ₂		22.7
Al ₂ O ₃		4.8
Fe ₂ O ₃		2.4
MgO		1.5
Na ₂ O		0.1
K ₂ O		0.8
SO ₃		0.5
XRD		Calcite Quartz Muscovite Chlorite

To perform the sandwich test, the coating agent was placed between the upper and bottom portion of brick sample with $55 \times 36 \times 36 \text{ mm}^3$ dimensions each piece and wrapped with a tape. A dead weight of 690 g was applied on top of the sandwich, which is equivalent to a load of 5.3 kPa, and then the sandwiches were introduced in the electric furnace. The coating test was carried out at 1500 °C for 5 h and during the cooling down step, the rate of 50 °C/h was applied below 1000 °C to prevent $\gamma\text{C}_2\text{S}$ formation.

The adherence strength of the clinker was considered as the average value of the cold modulus of rupture (CMOR) performed after the sandwich test, using ISO 13765-4: 2012 standard. After the CMOR test, some clinker–brick interfaces were analyzed by means of optical microscopy, scanning electron microscopy (Jeol, JSM-7100FLV model) coupled with energy dispersive X-ray spectrometer (Aztec Energy using X-Max 80 detector), and X-ray microtomography (micro-CT scanner of Bruker SkyScan 1174, with 50 kV source voltage, 800 µA source current and 10.03 µm image pixel size) using a 1 mm aluminum filter. In the latter test, samples of $8.5 \times 8 \times 6 \text{ mm}^3$ were attached to a stage that rotated 180° with images acquired at every 0.7°. The acquired shadow projections (16-bit TIFF format) were further reconstructed into 2D slices using the NRecon software interface

(v.1.7.4.6, Skyscan, Bruker micro-CT, Belgium). Quantitative analyses were made using CTAn software (v.1.18.8.0, Bruker micro-CT, Belgium) and CTVox software (v.3.3.0, Skyscan, Bruker micro-CT, Belgium) was used for 3D volumetric visualization.

3. Results and Discussion

3.1. Characterization of Magnesia–Spinel Brick Compositions

Tables 3 and 4 show the properties of A-1 to A-10 compositions. Overall, the increase in the firing temperature affected all properties, contributing positively to an increase in bulk density, hot modulus of rupture at 1485 °C and permeability, and to a decrease in apparent porosity and modulus of elasticity.

Table 3. Properties of magnesia–spinel brick compositions fired at 1500 °C.

Brick	A-1	A-2	A-3	A-4	A-5
BD (g/cm ³)	2.98	2.98	2.96	2.99	3.00
AP (%)	14.7	14.6	14.3	14.8	14.9
ME (GPa)	34	30	31	30	31
CCS (MPa)	86	83	70	84	90
HMOR at 1200 °C-3 h (MPa)	8.6	8.4	4.5	9.2	10.0
HMOR at 1485 °C-3 h (MPa)	1.8	1.5	0.5	1.0	2.0
Permeability (cD)	18	18	32	29	21
Chemical Composition (wt.%)					
MgO	87.6	84.8	85.0	83.5	86.1
Al ₂ O ₃	11.0	13.8	12.4	12.8	10.0
CaO	0.8	0.7	1.8	0.8	0.8
SiO ₂	0.2	0.2	0.2	0.2	0.3
Fe ₂ O ₃	0.4	0.4	0.4	2.5	0.4
ZrO ₂	0.0	0.0	0.0	0.0	2.1
XRD	MgO	MgO	MgO	MgO	MgO
	MA	MA	MA	MA	MA
	β C ₂ S	β C ₂ S	Q phase	MA	Cub. ZrO ₂
			C ₁₂ A ₇	MF	CaZrO ₃

Table 4. Properties of magnesia–spinel brick compositions fired at 1700 °C.

Brick	A-6	A-7	A-8	A-9	A-10
BD (g/cm ³)	2.98	2.99	2.98	2.99	3.03
AP (%)	14.5	14.4	13.5	14.3	14.0
ME (GPa)	28	22	31	25	27
CCS (MPa)	88	74	54	83	86
HMOR at 1200 °C-3 h (MPa)	7.0	6.4	6.1	7.8	7.6
HMOR at 1485 °C-3 h (MPa)	1.4	1.7	0.7	1.3	2.4
Permeability (cD)	35	35	48	46	59
Chemical Composition (wt.%)					
MgO	87.2	86.4	87.1	83.9	84.0
Al ₂ O ₃	11.1	12.1	10.4	12.4	12.3
CaO	0.8	0.7	1.7	0.8	0.8
SiO ₂	0.2	0.2	0.2	0.2	0.2
Fe ₂ O ₃	0.4	0.4	0.4	2.6	0.5
ZrO ₂	0.0	0.0	0.0	0.0	2.0
XRD	MgO	MgO	MgO	MgO	MgO
	MA	MA	MA	MA	MA
	β C ₂ S	β C ₂ S	Q phase	MF	Cub. ZrO ₂
					CaZrO ₃

It is obvious that the higher the firing temperature, the more liquid forms, enhancing properties such as density and porosity. However, the permeability also increased which may be related to the pore size growth that results from pore coalescence with sintering

process. Permeability is considered the most important physical property of magnesia–spinel refractory bricks which affects coatability, since it can promote clinker infiltration and contribute to a physical coating adherence. At the same time, it is observed that the use of high firing temperature decreased the cold crushing strength for calcined alumina and limestone additions, and hot modulus of rupture at 1200 °C for all additions.

Similarly to increasing firing temperature, the use of additives also influenced all properties. Zirconia contributed positively to increase in bulk density, hot modulus of rupture at 1200 °C and 1485 °C, and permeability, which suggests that this addition is beneficial to the sintering and densification, as also observed by Meng et al. [11]. On the contrary, limestone has a negative effect on these properties, except in increasing permeability. Due to the formation of in situ spinel, the addition of calcined alumina strongly reduces the modulus of elasticity of the refractory. The greatest effect of the hematite addition was the increase in permeability.

As expected, there was an increase in the corresponding oxide in the chemical composition when the additives were used. In general, when 2 wt.% of calcined alumina was added to the composition, the Al_2O_3 content increased from 11.0 to 13.0 wt.%. For the addition of 2 wt.% of limestone, the CaO content increased from 0.8 to 1.8 wt.%, and for the addition of 2 wt.% of hematite, the Fe_2O_3 content increased from 0.4 to 2.6 wt.%. When 2 wt.% of zirconia was added, the ZrO_2 content increased from 0 to 2.0 wt.% since this oxide was not originally present in the raw materials.

The XRD patterns are illustrated in Figures 1 and 2. The additives were recognized through the presence of mayenite and Q phase (for limestone), magnesium ferrite (for hematite), cubic zirconia and calcium zirconate (for CaO-partially stabilized zirconia). The presence of mayenite (C_{12}A_7) and Q phase ($\text{Ca}_{20}\text{Al}_{26}\text{Mg}_3\text{Si}_3\text{O}_{68}$) means that the spinel from the brick reacted with calcium oxide from limestone, forming these low refractoriness phases ($T_{\text{mp}} = 1390$ °C for C_{12}A_7 , $T_{\text{mp}} = 1300$ to 1400 °C for Q phase [15]). Therefore, the addition of limestone contributes to the formation of more liquid phases, resulting in the drop of hot properties obtained by A-3 and A-8 compositions. Part of the added zirconia reacted with the calcium oxide from the raw materials to form calcium zirconate (CaZrO_3), a very refractory material ($T_{\text{mp}} = 2340$ °C) what justifies the enhance in hot properties. For calcined alumina addition, no new phases were detected, which means that all alumina reacted with magnesia in the matrix, forming in situ spinel.

Figures 3 and 4 illustrate the microstructure of A-1 to A-10. All compositions presented homogeneous distribution of magnesia and fused spinel raw materials. Good sintering degree was obtained by A-4, A-6, A-7, A-9 and A-10 compositions. A refractory structure with a suitable sintering degree presents larger bonds among the particles, which may easily promote the reaction with clinker phases to form the coating. The addition of limestone to A-3 and A-8 resulted in partial corrosion of fused spinel and excessive sintering degree, which is related to the formation of C_{12}A_7 and Q phase. The other compositions (A-1, A-2 and A-5), fired at 1500 °C, presented reasonable sintering degree.

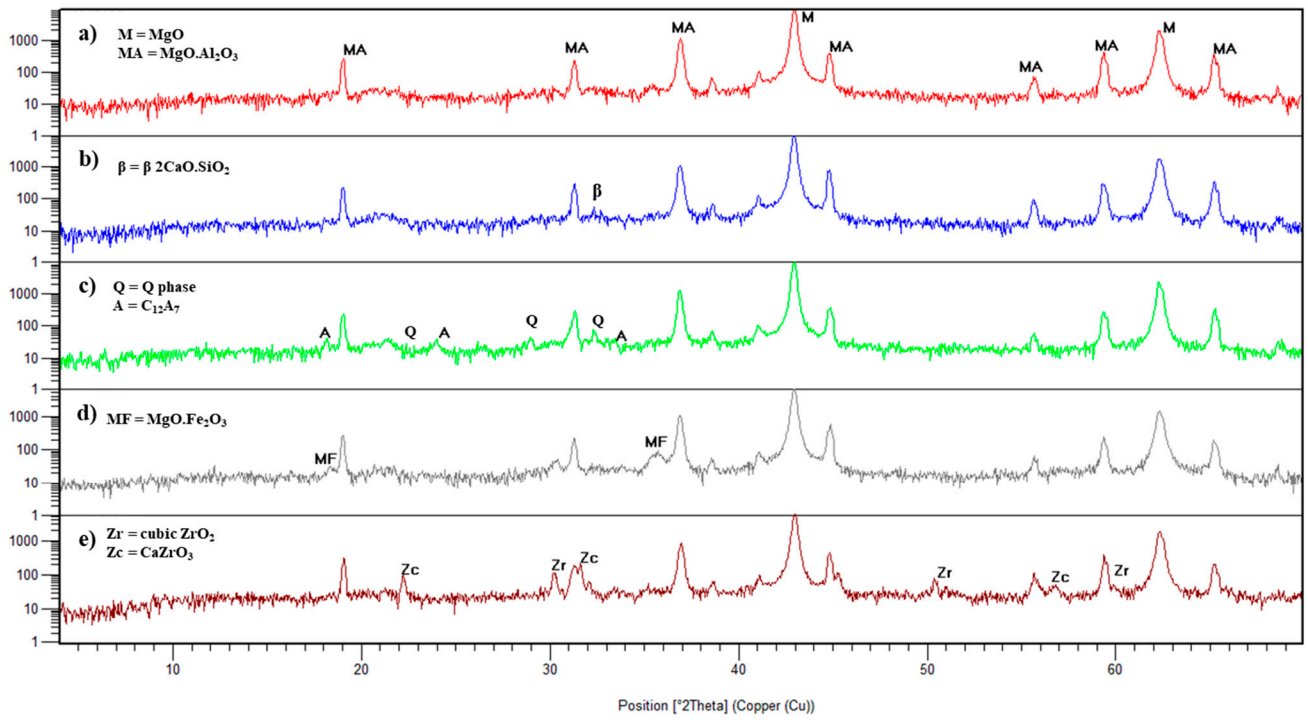


Figure 1. X-ray diffraction patterns of compositions (a) A-1, (b) A-2, (c) A-3, (d) A-4 and (e) A-5.

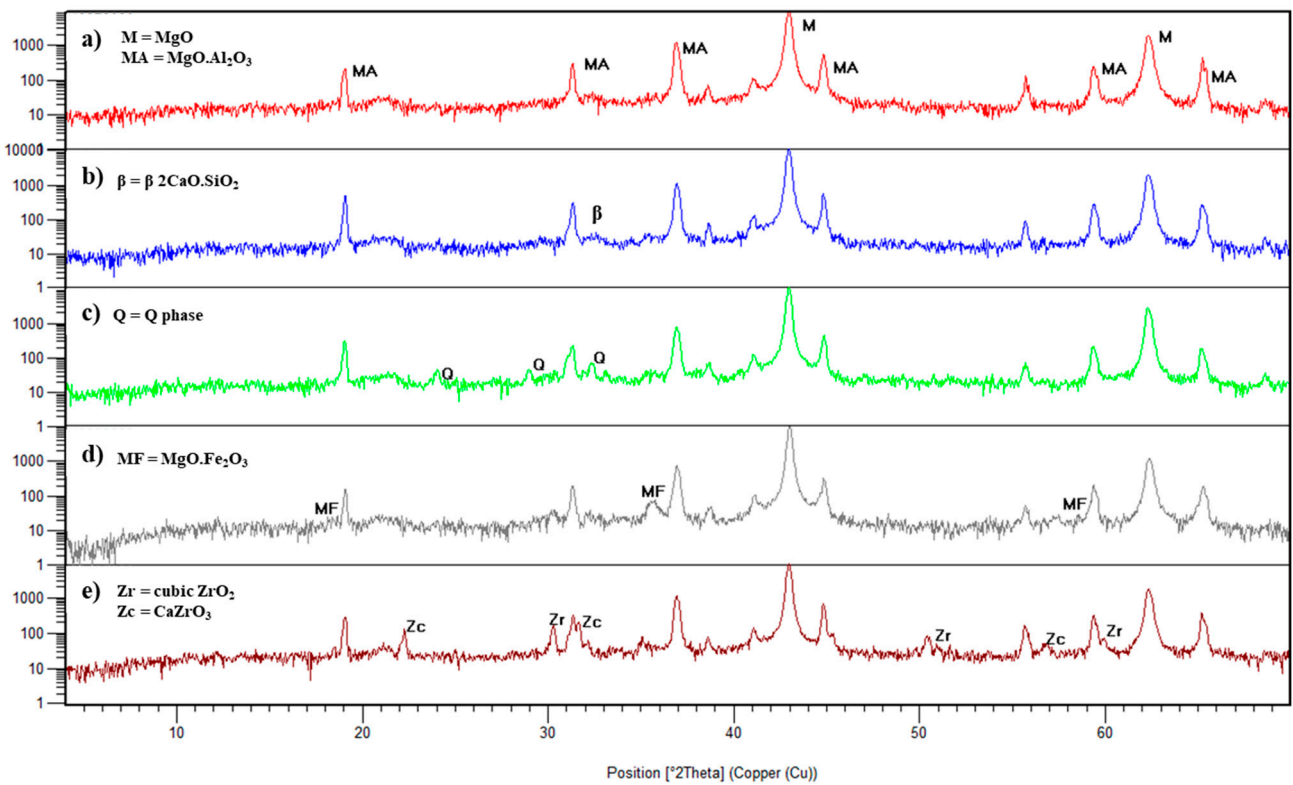


Figure 2. X-ray diffraction patterns of compositions (a) A-6, (b) A-7, (c) A-8, (d) A-9 and (e) A-10.

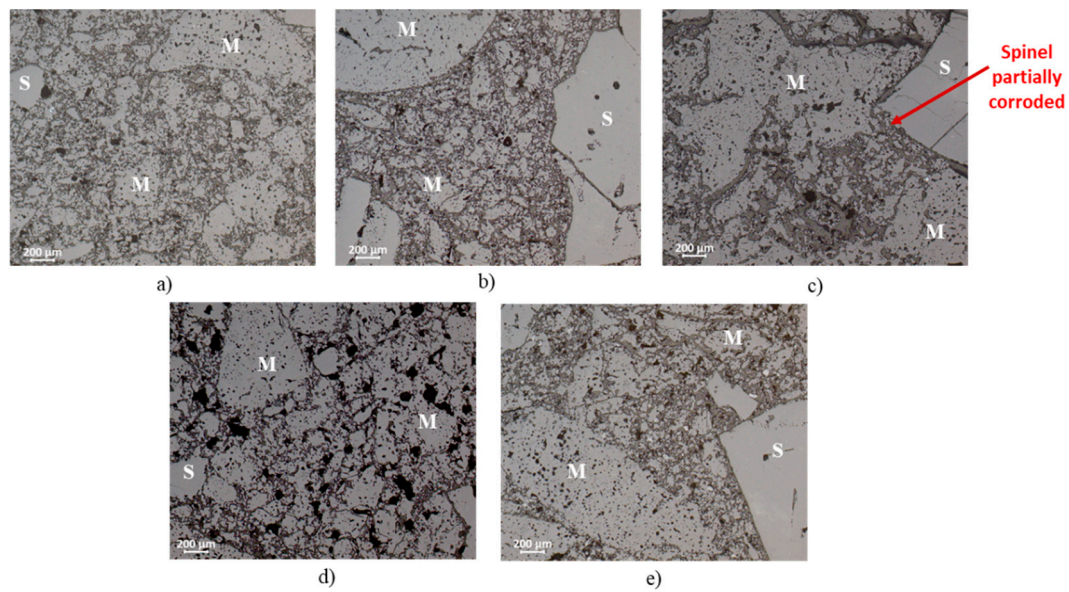


Figure 3. Microstructure of compositions (a) A-1, (b) A-2, (c) A-3, (d) A-4 and (e) A-5 (M = magnesia, S = fused spinel)—50× magnification.

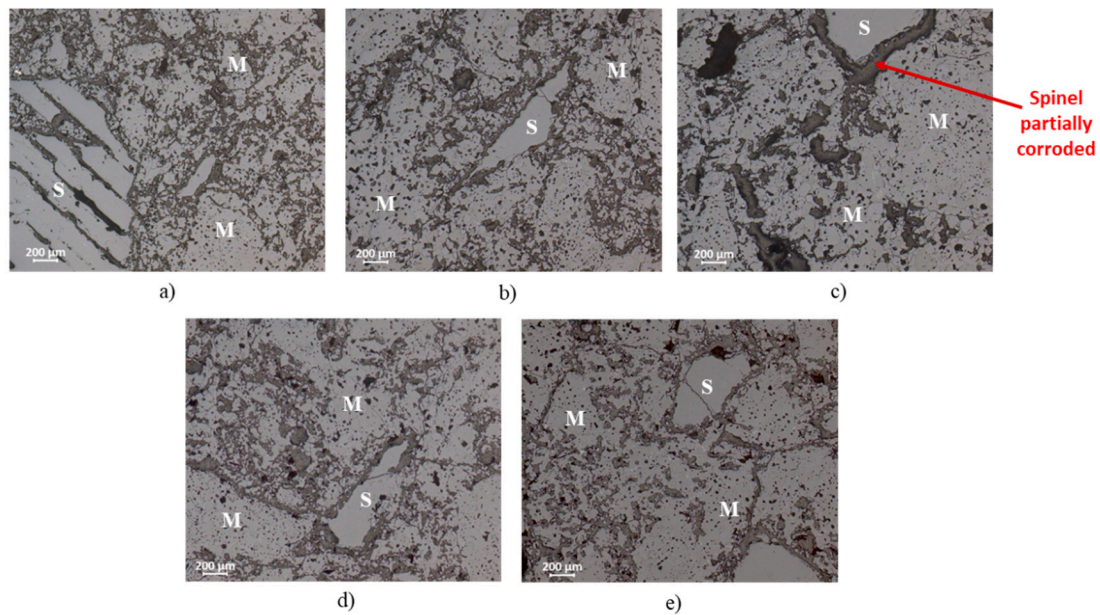


Figure 4. Microstructure of compositions (a) A-6, (b) A-7, (c) A-8, (d) A-9 and (e) A-10 (M = magnesia, S = fused spinel)—50× magnification.

3.2. Coating Test

The evaluation of the coating adherence ability by the sandwich coating test for A-1 to A-10 compositions is described in Figure 5. The highest coating strength was obtained by A-3 (limestone and 1500 °C), which presented 3.3 MPa in cold modulus of rupture test. This composition was followed by A-8 (limestone and 1700 °C), with 2.9 MPa, and A-6 (no additions and 1700 °C), with 2.7 MPa. These values match the results between 0 and 4 MPa obtained by Guo et al. [3], and the results between 0 to 1.4 MPa obtained by Lin et al. [12], using the sandwich coating test.

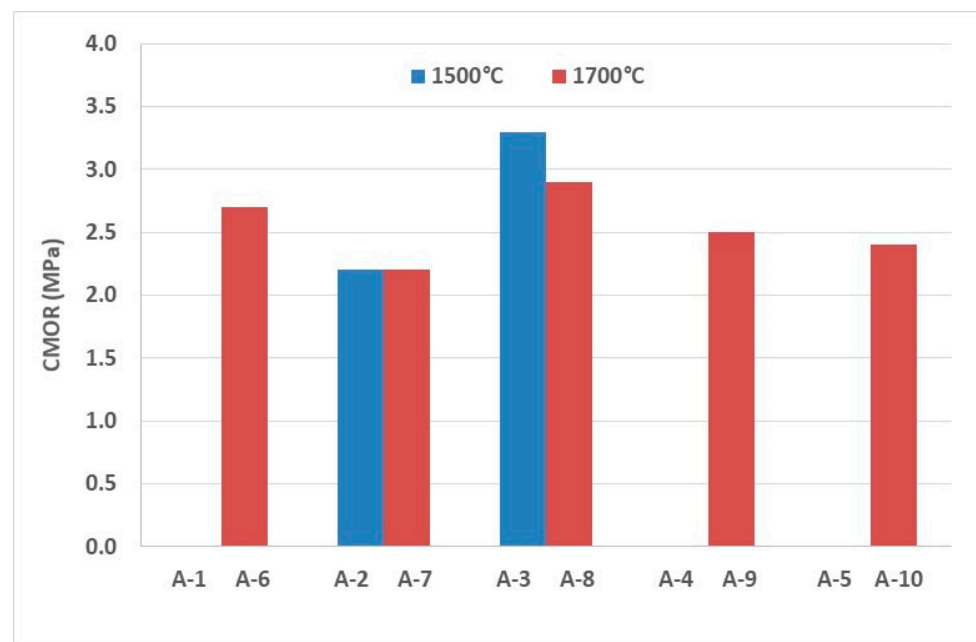


Figure 5. Cold modulus of rupture of magnesia–spinel brick compositions after the sandwich coating test.

There are two common features when comparing the three best compositions in terms of coating: addition of limestone and high firing temperature. The calcium from limestone addition reacts with spinel from the brick, forming low refractoriness phases and contributing to liquid phase formation which is essential to the coating adherence on magnesia–spinel bricks. Mayenite ($C_{12}A_7$) and Q phase ($Ca_{20}Al_{26}Mg_3Si_3O_{68}$) were identified in XRD of the compositions with limestone, in addition to partial corrosion of fused spinel grains observed in the microstructure. The use of high firing supports the migration of impurities in the raw materials to the liquid phase of the refractory, as well as guaranteeing a well-sintered refractory structure and increased permeability, all contributing positively to the coating adherence. It must be pointed out that A-3, A-6 and A-8 compositions showed permeability higher than 30 cD and good to excessive sintering degree.

It is observed that the addition of hematite and zirconia to magnesia–spinel bricks in order to improve coating adherence is only effective if combined with high firing temperature. High firing temperature is important to elevate permeability and to improve sintering degree, leading to optimal coating adherence, as previously discussed. Moreover, when adding zirconia, part of it reacts with calcium oxide from the brick and another part reacts with lime phases from the clinker, forming calcium zirconate ($CaZrO_3$) and helping the formation of a protective coating [8,9,16]. In the case of hematite addition, the formation of magnesium ferrite contributes to the liquid phase formation, which is essential for adhering coating on magnesia–spinel bricks [3]. Tokunaga et al. [7] had also observed coating stability by the addition of pure iron oxides.

However, for calcined alumina and limestone additions, the increase in the firing temperature did not significantly change the coating strength. It is easily understood that the addition of calcined alumina increases the spinel content and promotes the formation of more liquid phase. This is in line with the results obtained by Lin et al. [12], where the greater the spinel content, the higher the content and the viscosity of the liquid phase, affecting the adherence property for compositions with spinel content lower than 50 wt.%. As in situ spinel is totally formed after firing at 1500 °C, there was no improvement with the increase in firing temperature. For limestone, the same conclusions are made, but the increase in the liquid phase is due to the presence of Q phase.

3.3. Microstructure Observations

The clinker–brick interface of A-1 and A-3 compositions were selected to be observed under optical microscope after the sandwich coating test, as they represent extreme cases of coating strength. Figure 6 shows that there are two different zones for A-1 (changed area and unaltered area) and three zones for A-3 (coating, changed area and unaltered area). Both microstructures were infiltrated by clinker liquid phase but to a lesser extent for A-1. Stable coating adherence on the brick surface, with 1500 μm thickness, is noticed only for A-3. After the altered area, the microstructure is typical for A-1 and A-3 compositions. Pictures with higher magnification were taken at the clinker–brick interface, as highlighted in Figure 7.

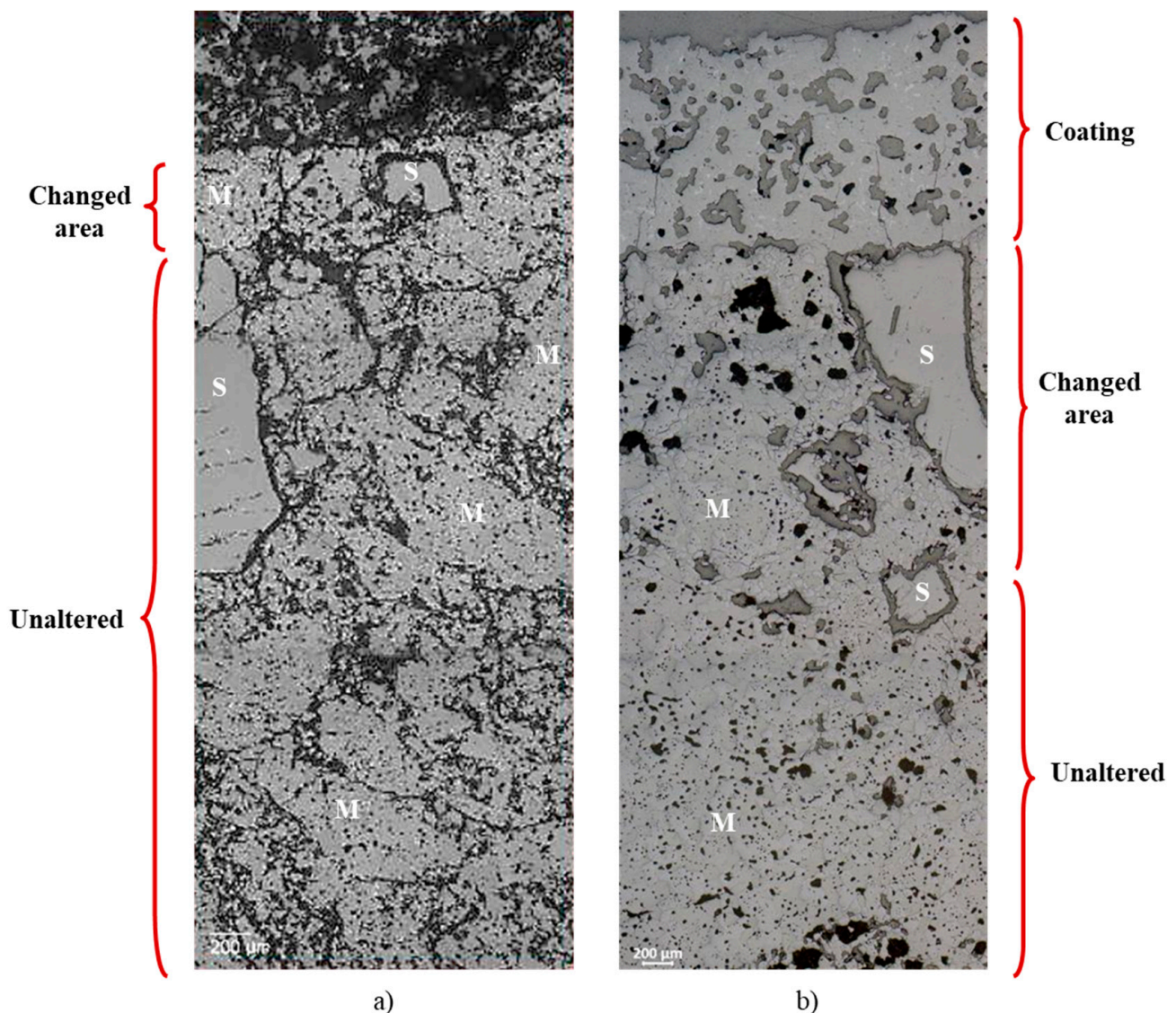


Figure 6. Microstructure of the clinker–brick interface of composition (a) A-1 (b) A-3 after the sandwich coating test (M = magnesia, S = fused spinel)—50 \times magnification.

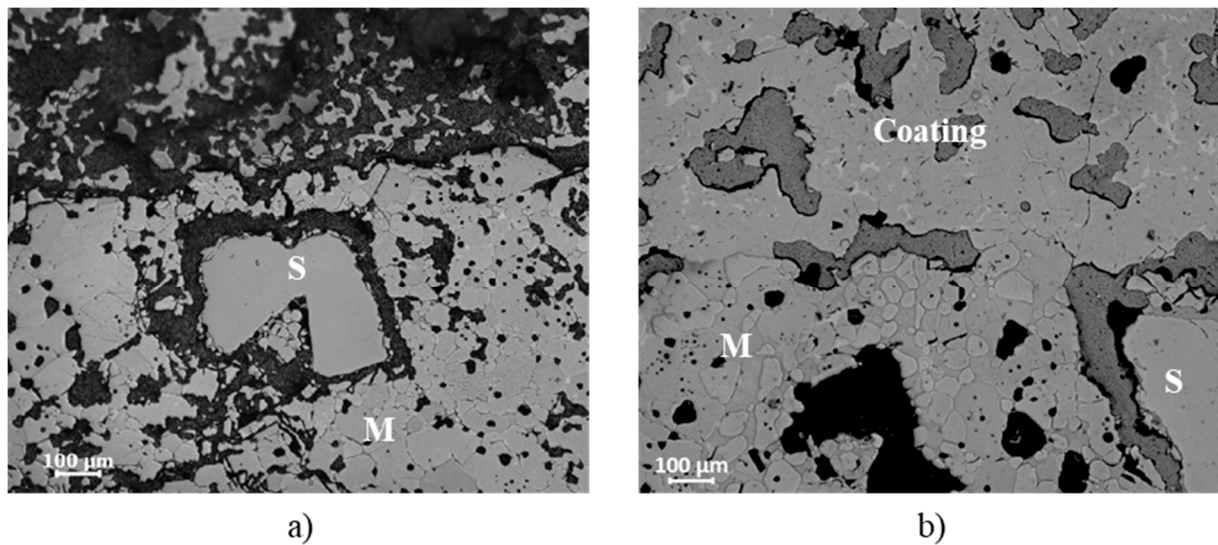


Figure 7. Microstructure of the clinker–brick interface of composition (a) A-1 (b) A-3 after the sandwich coating test (M = magnesia, S = fused spinel)—100× magnification.

A partial corrosion of the fused spinel by clinker phases can be observed in the area just below the interface for both compositions, but the disintegration of magnesia grains is more evident for A-3. Although magnesia did not react with clinker phases, it is dissolved by the liquid composed of the main oxides present in the clinker, namely, CaO, SiO₂, Al₂O₃ and Fe₂O₃, which is analogous to a sintering process in the presence of liquid phase [3,6]. Bonding is also noticed between magnesia grains and coating in the microstructure corresponding to the A-3 composition.

The SEM-EDS analysis of the selected interfaces after the sandwich test is illustrated in Figure 8. The mapping of the region shows the distribution of chemical elements that constitute the coating and brick areas in different colors. It is observed, for A-1 composition, that elements Ca, Si and O are predominant at the top part corresponding to the coating area, and elements Mg and O are predominant at the bottom part corresponding to the brick area. For A-3, element Al is also present in the coating area, in addition to Ca, Si, and O. In the brick area, elements Mg and O are predominant in the grains, and Ca, Si, Al and O are predominant in the liquid phase permeating through the grains.

Because no expressive amount of Al and, therefore, liquid phase, was detected in the clinker and brick areas for A-1, higher magnification in the interface with chemical composition by EDS for phase identification was carried out. Figure 9 shows that in the clinker area of A-1, only phases C₂S and C₃A were identified. No elements and phases were detected in the grain boundaries. In the brick, MgO grains are predominant, but a small area with C₂S and spinel was also observed. Thus, the absence of liquid phase in both areas explains the low coating adherence observed for A-1 composition. On the contrary, there are at least two different types of liquid phase in the clinker area of A-3: one more predominant and richer in C₃A (point 1), and another one located in the dark grey pockets and richer in Q phase (points 3 and 5), as illustrated in Figure 9. In the brick area, two different liquid phase compositions were also identified, richer in C₂S (point 6) and richer in Q phase (point 7).

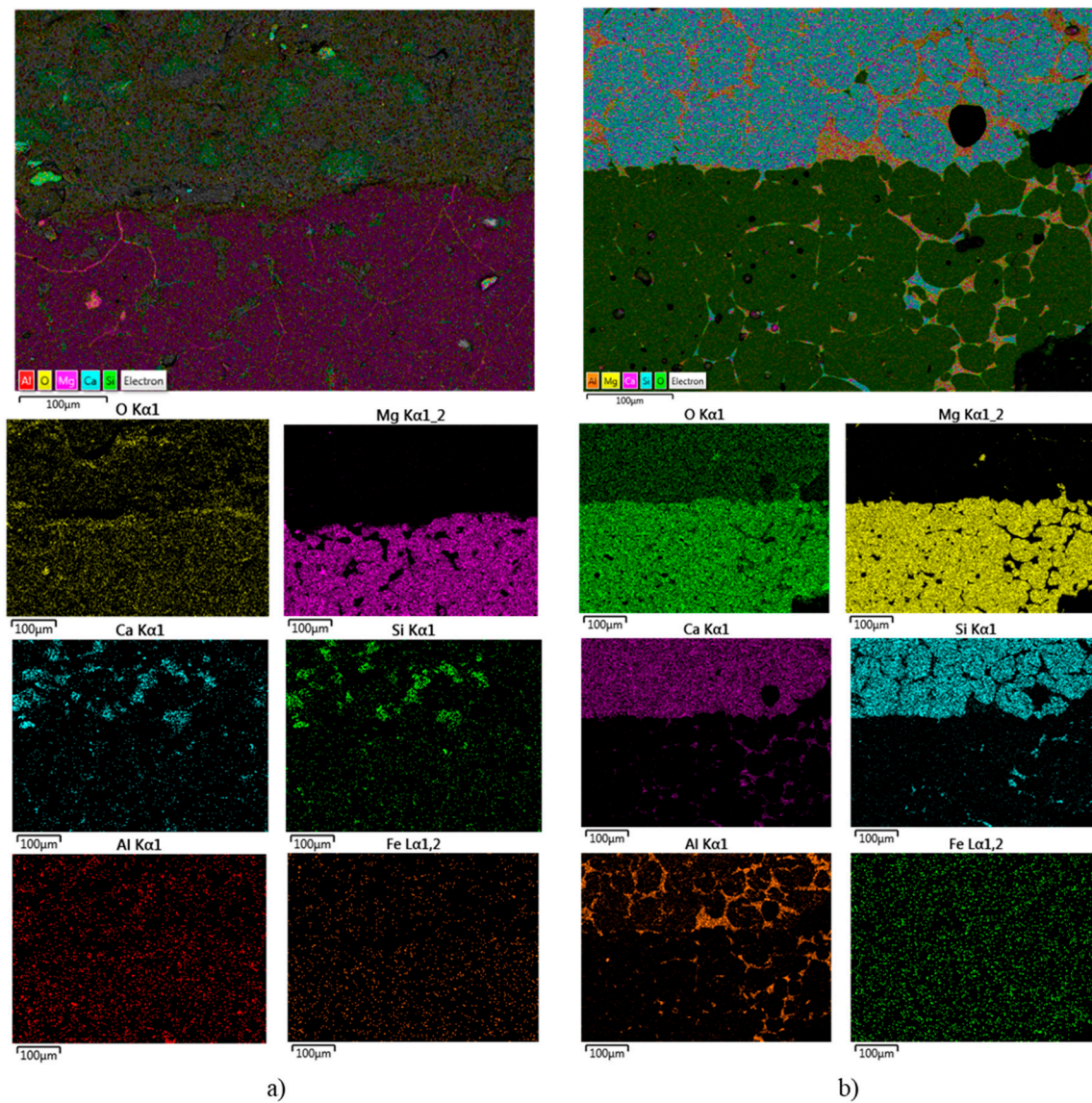


Figure 8. SEM micrograph of the clinker–brick interface of composition (a) A-1 (b) A-3 after the sandwich coating test—200× magnification.

These analyses demonstrate that the liquid phase at the clinker–brick interface of A-3 composition is composed of brick and clinker components as a result of the reaction between them. Therefore, the resulting liquid phase is the link between the clinker and the brick, and it is essential to form coating in magnesia–spinel bricks. For A-1, SEM analysis did not show an abundant liquid phase, and consequently, no coating was adhered to the brick surface.

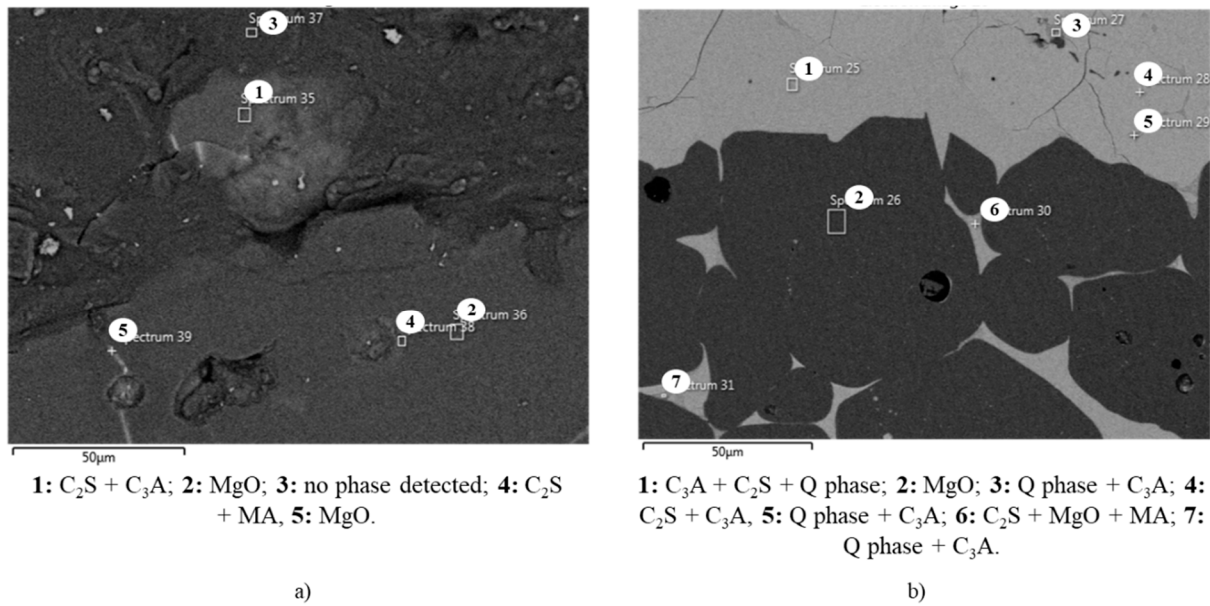


Figure 9. SEM micrograph of the clinker–brick interface of composition: (a) A-1, (b) A-3 after the sandwich coating test—700× magnification.

3.4. Micro-CT Analysis

For visual observation of the effect of coating formation on magnesia–spinel bricks, A-1 and A-3 compositions were again selected to be examined by means of X-ray microtomography (micro-CT) after the sandwich coating test. Micro-CT is a non-destructive method that provides 3D images of the internal structure of a material at a spatial resolution better than 1 micrometer [17]. During the exposition, X-rays interact with the sample and are attenuated depending on the density of the material, the sample size, the atomic number of the elements as well as the wavelength of the X-rays [18]. In general, for a fixed X-ray photon energy, elements with lower atomic number absorb less than elements with higher atomic number [17].

Figure 10 presents the 3D model reconstruction of the coating and the brick areas, and the pore size distribution histogram of the brick area for both samples. The structural differences in the image for A-3, which presented the coating adhered to the surface, can be observed. It is possible to identify the interconnectivity between clinker and brick due to the difference in brightness, which is a function of the atomic number (Z) of the absorbing element in each area. As coating is mainly rich in Ca ($Z = 20$) and Si ($Z = 14$), whose atomic numbers are higher compared to Mg ($Z = 12$) and Al ($Z = 13$) in the brick area, it presents greater X-ray attenuation resulting in the formation of contrast in the micro-CT images represented by the lighter region. On the other hand, A-1 did not present adhered coating, so no lighter region is observed.

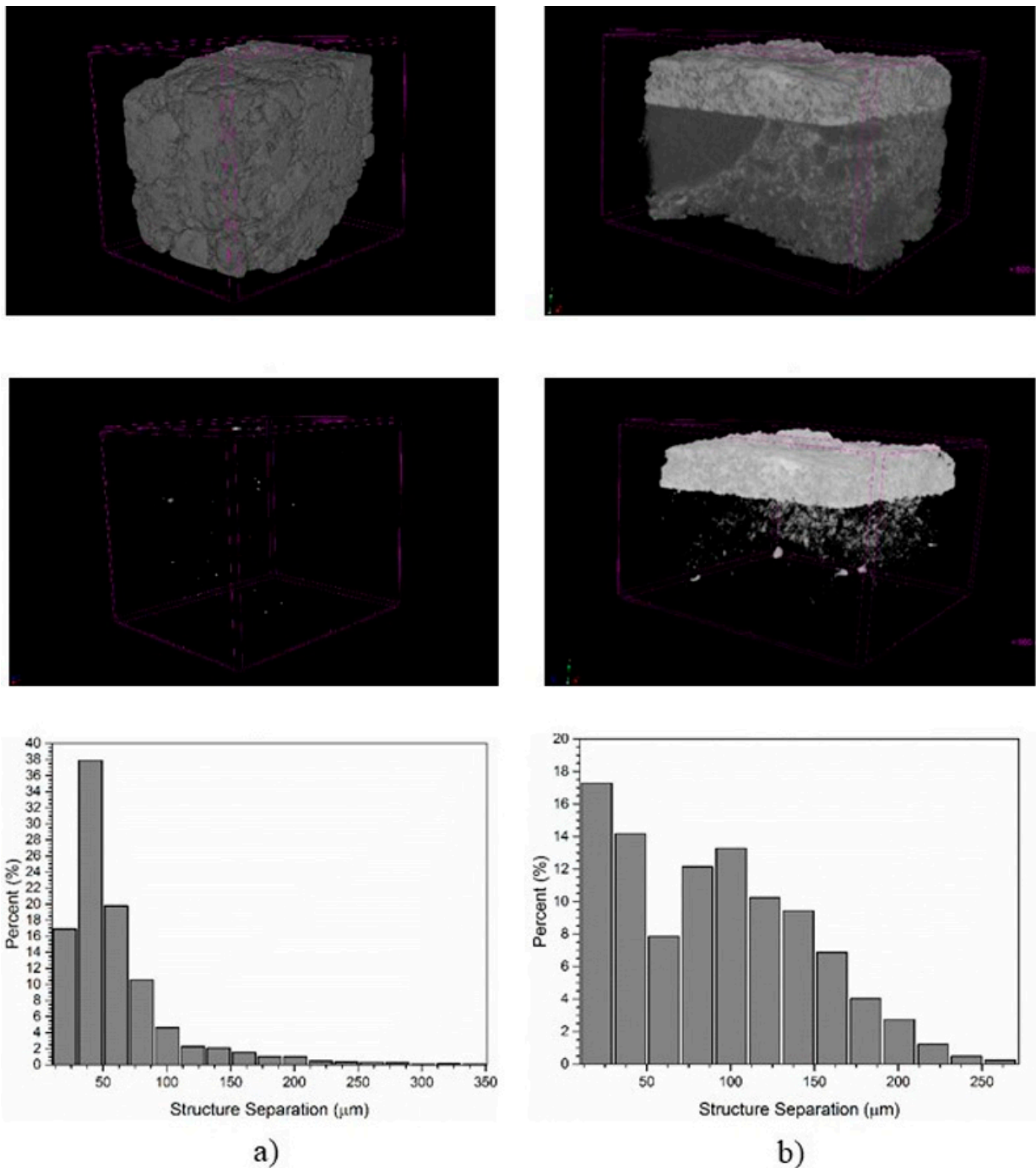


Figure 10. 3D images and pore size distribution of the brick area obtained by micro-CT of composition: (a) A-1 and (b) A-3 after the sandwich coating test.

The pore size distribution histogram shows that A-3 presented broader distribution with pore size smaller than $250\ \mu\text{m}$, whereas for A-1, a narrow distribution is observed, with most of the pores below $100\ \mu\text{m}$, but more concentrated at the order of $25\text{--}50\ \mu\text{m}$. The total porosity was calculated at 20.4% for A-1, with an average pore size of $62.2\ \mu\text{m}$, whereas A-3 presented 19.7% total porosity and $90.9\ \mu\text{m}$ average pore size. Although they present similar total porosity, the higher average pore size of A-3 implies greater permeability, which seems to be essential to adhere coating to magnesia–spinel bricks.

4. Conclusions

This investigation was able to enhance the adherence ability of coating on magnesia–spinel refractory bricks varying the additives and firing temperature used. During the work, it was possible to confirm, with the selected clinker composition, that the coating formation and adherence on the brick surface depend on physical and chemical interaction between the clinker and the brick.

The physical interaction was facilitated when the permeability of the refractory was elevated and when it presented good sintering degree, mainly due to the use of high firing temperature. These characteristics demonstrated great importance to improve coatability, since high permeability promotes clinker infiltration, whereas suitable sintering degree promotes the contact of refractory particles with the clinker phases.

For chemical interaction, it has been demonstrated that the formation of liquid phase is essential to adhere coating. In this way, the addition of 2 wt.% of limestone was the most efficient to improve the coating strength from 0 MPa to 3 MPa of a typical magnesia–spinel brick. However, this addition resulted in a drop in hot modulus of rupture at 1200 °C and 1485 °C because of the presence of $C_{12}A_7$ and Q phase. Thus, alternative compositions which combine good adherence and hot properties would be preferably those with higher firing temperature and maintaining a high level of purity of the refractory.

Therefore, it can be said that it is possible to improve the coatability of magnesia–spinel bricks through the design of their composition.

Author Contributions: Conceptualization, G.R.C.P., G.E.G. and V.d.F.C.L.; methodology, G.R.C.P. and G.E.G.; validation, G.R.C.P. and G.E.G.; investigation, G.R.C.P.; writing—original draft preparation, G.R.C.P.; writing—review and editing, G.R.C.P., G.E.G. and V.d.F.C.L.; visualization, G.R.C.P.; supervision, G.E.G. and V.d.F.C.L.; project administration, G.R.C.P. and V.d.F.C.L. All authors have read and agreed to the published version of the manuscript.

Funding: This research received financial support of Conselho Nacional de Desenvolvimento Científico e Tecnológico, CNPq, grant number 306291/2018-5 to Vanessa Lins.

Institutional Review Board Statement: Not applicable.

Informed Consent Statement: Not applicable.

Acknowledgments: The authors are grateful to RHI Magnesita, for providing the infrastructure for this work, and CNPq. We thank Breno Barrioni and Marivalda Pereira for performing micro-CT analysis, and Lourdes Pinto and Diana Escobar for SEM analysis.

Conflicts of Interest: The authors declare no conflict of interest.

References

1. Griffin, D.; Knauss, R. New developments in fired doloma bricks used in rotary cement kilns. In Proceedings of the Unified International Technical Conference on Refractories (UNITECR), Salvador, Brazil, 13–16 October 2009.
2. Guo, Z.; Palco, S.; Rigaud, M. Bonding of Cement Clinker onto Doloma-Based Refractories. *J. Am. Ceram. Soc.* **2005**, *88*, 1481–1487. [[CrossRef](#)]
3. Guo, Z.; Palco, S.; Rigaud, M. Reaction Characteristics of Magnesia–Spinel Refractories with Cement Clinker. *Int. J. Appl. Ceram. Technol.* **2005**, *2*, 327–335. [[CrossRef](#)]
4. Sengupta, P. *Refractories for the Cement Industry*; Springer: Cham, Switzerland, 2020; pp. 185–192.
5. Brito, C.; Reis, E.M. Doloma brick benefits. *Int. Cem. Rev.* **2015**, 99–102.
6. Rigaud, M.; Guo, Z.; Palco, S. Coating formation on basic bricks in rotary cement kilns. In Proceedings of the Asociación Latinoamericana de Fabricante de Refractarios (ALAFAR), Pucón, Chile, 5–7 December 2000.
7. Tokunaga, K.; Kozuka, H.; Honda, T.; Tanemura, F. Further improvement in high temperature strength, coating adherence, and corrosion resistance of magnesia–spinel bricks for rotary cement kiln. In Proceedings of the Unified International Technical Conference on Refractories (UNITECR), Aachen, Germany, 23–26 September 1991.
8. Kozuka, H.; Kijita, Y.; Tokunaga, K.; Sakakbara, K.; Ohta, S. Further improvement of MgO–CaO–ZrO₂ bricks for burning zone of rotary cement kiln. In Proceedings of the Unified International Technical Conference on Refractories (UNITECR), Kyoto, Japan, 19–22 November 1995.
9. Ukawa, S.; Arai, M.; Inoue, S.; Azuma, T.; Sakai, R.; Shikama, S. The application of chrome-free bricks with improved coating adhesion for cement rotary kilns. *J. Tech. Assoc. Refract.* **2009**, *29*, 122–128.

10. Chen, J.; Yan, M.; Su, J.; Li, B.; Sun, J. The kiln coating formation mechanism of MgO-FeAl₂O₄ brick. *Ceram. Int.* **2016**, *42*, 569–575. [[CrossRef](#)]
11. Meng, W.; Ma, C.; Ge, T.; Zhong, X. Effect of zircon addition on the physical properties and coatability adherence of MgO–2CaO.SiO₂–3CaO.SiO₂ refractory materials. *Ceram. Int.* **2016**, *42*, 9032–9037. [[CrossRef](#)]
12. Lin, X.; Yan, W.; Ma, S.; Chen, Q.; Li, N.; Han, B.; Wei, Y. Corrosion and adherence properties of cement clinker on porous periclase-spinel refractory aggregates with varying spinel content. *Ceram. Int.* **2017**, *43*, 4984–4991. [[CrossRef](#)]
13. Pacheco, G.; Gonçalves, G.E.; Lins, V. Qualitative and Quantitative coating tests: A comparison in Magnesia–Spinel Refractory Bricks. *Ceramics* **2020**, *3*, 144–154. [[CrossRef](#)]
14. Zhao, M. Quantitative Control of C₂S Crystal Transformation. *Appl. Mech. Mat.* **2012**, *121*, 311–315. [[CrossRef](#)]
15. Wajdowicz, A.; Gonçalves, G.E.; Pacheco, G.R.C.; Pinilla, J.; Oliveira, M.G.; Brito, M.A.M. Magnesia-spinel brick: A Thermal Overload Case. In Proceedings of the 54th International Colloquium on Refractories, Aachen, Germany, 19–20 October 2011.
16. Guotian, Y.; Yanqing, X. ZrO₂ containing Refractories for Cement Rotary Kilns. *China's Refract.* **2002**, *11*, 13–16.
17. Landis, E.N.; Keane, D.T. X-ray microtomography. *Mat. Charact.* **2010**, *61*, 1305–1316. [[CrossRef](#)]
18. Hubalkova, J.; Silva, W.M.; Aneziris, C.G. X-ray computed tomography as a tool for investigation of refractories. In Proceedings of the 53rd International Colloquium on Refractories, Aachen, Germany, 8–9 September 2010.